IEEE Access
Multidisciplinary | Rapid Review | Open Access Journal

Received 4 July 2024, accepted 13 August 2024, date of publication 16 August 2024, date of current version 28 August 2024.

Digital Object Identifier 10.1109/ACCESS.2024.3445159

RESEARCH ARTICLE

Optimal Arrangement of Power Cables in Ducts Using the Agamogenetic Algorithm

RUNZE CAI AND SHIYOU YANG, (Senior Member, IEEE)
College of Electrical Engineering, Zhejiang University, Hangzhou 310027, China
Corresponding author: Runze Cai (11910069@zju.edu.cn)

ABSTRACT Duct bank installation, as a popular installation type for underground power cables, has been widely used. However, laying excessive number of ducts in a duct bank has given rise to the cable arrangement problem. Meanwhile, the current academic research on the cable arrangement problem is not mature. In this regard, this paper proposes a novel stochastic optimization algorithm namely the agamogenetic algorithm to solve the cable arrangement problem. The roulette strategy is applied in the mutation process of the proposed algorithm, leading to the development of two novel operators, namely the excitation operator and the interchange operator. From the general agamogenetic algorithm, this paper further designs its customized variants for the two-ends and single-end grounding modes. Subsequently, the concept of cross-bonded grounding mode is promoted, and a cross-bonded configuration beyond the same transmission circuit is proposed, namely the generalized cross-bonded grounding mode. Due to its requirement to simultaneously optimize the cable arrangement and the sheath cross-bonded structure, a specific oriented agamogenetic algorithm is also designed. Finally, a real-life duct bank installation is used as the case study, validating that the agamogenetic algorithm has higher convergence speed, accuracy, and stability compared to existing algorithms for optimizing cable arrangements in ducts. Simulation results also show that the loss or voltage of the optimal arrangement decreases by 12.24%, 50.66%, and 11.67% under the two-ends, single-end, and cross-bonded grounding modes, respectively, compared to the standard engineering arrangement.

INDEX TERMS Cross-bonded grounding, duct, genetic algorithm, optimal arrangement, power cable.

I. INTRODUCTION

Over the past few decades in urbanization, the demand for electric energy has increased significantly. Due to overhead transmission lines affecting urban landscapes and occupying urban space, underground power cables become more preferable in urban distribution networks. One of the installation types of underground power cables is to put cables in nonmetallic ducts, as shown in Fig. 1. This installation type reduces the probability of cables being mechanically damaged and the corrosion to cables caused by harmful substances in the soil. At the same time, cables in ducts take up less underground space and have a lower cost as compared to the tunnel installation, and are more convenient to be renewed without digging the road as compared to the direct burying mode. Therefore, the duct bank installation has become the most widely used installation type in urban areas, particularly suitable for regions with dense underground pipelines or heavy traffics [1], [2], [3], [4], [5].

Nevertheless, the duct bank installation has a major disadvantage that it complicates the electromagnetic induction in the metal sheaths of cables. This significantly reduces the effectiveness of the cross-bonded grounding mode in suppressing circulating currents and controlling sheath voltages. Moreover, unexpected results may occur concerning sheath voltages and circulating currents under single-end and two-ends grounding modes. Therefore, traditional duct bank installation may lead to increased circulating currents and higher voltages to ground in metal sheaths. As is well known, excessive circulating currents in metal sheaths can result in increased joule losses and elevated temperatures, thereby reducing the current rating of the cable, accelerating

The associate editor coordinating the review of this manuscript and approving it for publication was Md. Abdur Razzaque.

© 2024 The Authors. This work is licensed under a Creative Commons Attribution-NonCommercial-NoDerivatives 4.0 License.
For more information, see https://creativecommons.org/licenses/by-nc-nd/4.0/

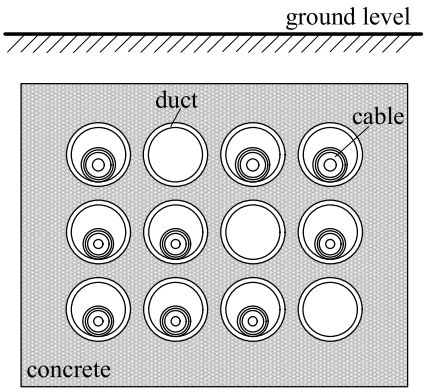

FIGURE 1. Schematic diagram of cables installed in a duct bank.

insulation aging, and shortening the cable lifespan. Additionally, it may induce significant voltages in the metal sheaths of nearby cables [6], [7], [8], [9], [10], [11]. Furthermore, excessive voltages in metal sheaths can lead to insulation breakdown and flashover at cable joints, potentially causing short-circuit faults [12], [13], [14], [15], [16]. However, it is observed that, for single-core power cables, different arrangements of cables in ducts can lead to remarkably different electromagnetic inductions in cable sheaths, indicating that there is an optimal cable arrangement corresponding to a specific goal such as minimizing the total cable losses or the maximum sheath voltage. In this regard, the optimization of cable arrangements in ducts is a research-worthy issue that has garnered the interest of the academic community. Some researchers have just explored the advantages and disadvantages of different types of cable layouts and grounding modes. Specifically, literature [17] recommends a linear arrangement for power cables to enhance dissipation, and a volumetric arrangement with internal separators for communication cables to reduce electromagnetic interference. Literatures [18], [19], [20], [21], [22] study the characteristics of flat and trefoil formations to guide cable installation under various operating conditions and environments. Building on the flat and trefoil formations, literature [23] further proposes inverted trefoil and vertical flat configurations to meet the heat dissipation requirements under unique installation conditions, and literature [24] further studies how the cable losses are influenced by the small trefoil, large trefoil and vertical layouts. Besides, studies have shown that increasing the cable spacing and using cross-bonded grounding mode and phase transposition can reduce sheath currents and voltages, thereby decreasing sheath losses and improving the current rating [21], [25], [26]. Nonetheless, the aforementioned research findings merely compare some of the most basic installation and laying forms, as well as grounding modes, of cables, and provide certain principles for cable layout and grounding under different operating conditions and laying environments. They do not constitute a true optimization of the arrangement for densely clustered power cables. In contrast, other researchers have investigated the optimal cable arrangement for maximizing the ampacities or minimizing the cable losses or some other goals by either selecting from the pre-given cable arrangements [27], [28], [29], [30], [31], [32], [33], [34] or exhaustively checking the possible arrangements to determine the optimal one [35], [36]. Among these, literatures [27], [28], [29], [30], [31] provide several candidate arrangements for duct bank installations. Literature [32] artificially proposes candidate arrangements involving different burial depths, positions, and crossing angles for multi-circuit cables in three-dimensional space. Literature [33] presents eight cable arrangements for three single-core cables operating in parallel with the same phase to screen for the optimal arrangement. Literature [34] discusses six different phase arrangements of the flat cable layout to search the optimal sequence impedance. However, these methods are just error and trial approaches, and cannot form an effective and instructive strategy for the optimization of cable installations in a duct bank. The commercial software CYMCAP can optimize the cable arrangements in ducts quickly. The optimization essence of this software is to optimize the heat dissipation conditions based on the thermal circuit model in IEC standards [37], [38], [39], [40], [41], thus it cannot minimize the joule losses in the metal sheaths, that is, it cannot optimize the heat sources. Moreover, when the optimization goal changes, such as optimizing the sheath voltages in the single-end grounding mode, this software is powerless.

Intuitively, the cable arrangement problem (CAP) is very similar to the travelling salesman problem (TSP) in that they both seek the optimal arrangement of a sequence of elements. Generally, a near-optimal solution to a large-scale TSP is obtained by using stochastic optimization algorithms such as genetic algorithms. The basic idea of genetic algorithms in solving the TSP is to retain and recombine critical information from the parent genetic structures to produce better offspring [42]. However, the CAP is fundamentally different from the TSP. If we define a path that passes through all the ducts, then the cable can represent the city in the TSP, and the sheath loss or other measures of the cable can represent its distance from adjacent cities. It is obvious that the ''distance'' between each two cables is not a constant, which will vary with the arrangement. This indicates that the arrangement fragments lack the ability to maintain traits. From this point of view, the genetic algorithms are not as effective in solving the CAP as they are in solving the TSP. Although literatures [43], [44] use genetic algorithms to optimize the phase arrangements and cable positions in a tunnel simultaneously, these optimization strategies only target the cable harness composed of three cables with different phases, and have no guiding significance for the single-core cable arrangement in ducts. Moreover, the direct application of genetic algorithms to optimize the arrangement of single-core cables will inevitably produce illegal arrangements. To address this issue, a customization of the standard genetic algorithm has been reported in [45] and [46], in which the crossover operator is removed, and only the mutation operator is retained to

conduct the iterative procedure. Since the retained mutation operator performs a completely random mutation and has no environmental tendency, the evolution efficiency of the reported strategy is not high.

Inspired by the genetic algorithm and the unique characteristics of the CAP, this paper proposes a novel stochastic optimization algorithm, named the agamogenetic algorithm, to efficiently obtain a near-optimal solution for the CAP. Utilizing the proposed algorithm, this paper further generalizes the standard cross-bonded grounding mode and optimizes its configuration to minimize cable losses. In the remainder of the paper, we provide a detailed description of the agamogenetic algorithm in Section II, as well as its customizations for two-ends and single-end grounding modes in Section III. Next, in Section IV, we propose the generalized cross-bonded grounding mode and search its optimal configuration by using the deeply customized version of the agamogenetic algorithm. Thereafter, in Section V, the optimization performance of the agamogenetic algorithm is validated with a real-life duct bank installation. Finally, conclusions are drawn in Section VI.

II. AGAMOGENETIC ALGORITHM IN SOLVING CABLE ARRANGEMENT PROBLEM

A. ENCODING AND DEFINITION

The number of cables per phase and for each load level must remain unchanged in different cable arrangements within the ducts. This feature implies that the existing crossover between two different arrangements is not applicable to the CAP, although special crossover operators can be designed to avoid the generation of illegal arrangements. In fact, cloning and mutation are naturally suitable for the CAP in the sense that the cloning ensures that the type and quantity of genetic material components remain unchanged while the mutation ensures that evolution can proceed. Based on cloning and mutation process, the so-called agamogenetic algorithm is constructed below. Before the construction of the proposed algorithm, the cable arrangement will be encoded and the concepts of gene, base and environmental capacity will be defined.

For the encoding of cable arrangements, firstly each cable is assigned a character to distinguish its phase and load level. For example, the character "A" represents the cable belonging to phase A of a heavy load circuit, and the character "b" represents the cable belonging to phase B of a light load circuit. No distinction is needed between the same-phase cables in different circuits with the same load level. If there is an empty duct, we use character "0" to represent this non-existent cable. After each cable is encoded by using a character, the gene of the agamogenetic algorithm in solving the CAP can be seen as the arrangement itself, which is a two-dimensional character matrix, as illustrated in Fig. 2(a). For the convenience of programming and representation, we map this two-dimensional character matrix into a one-dimensional character chain in a specific order, as illustrated in Fig. 2(b). The number at the top of each duct represents the position index within the character chain going from left to right. Therefore, the gene representing each arrangement is defined as the corresponding sequence of characters. Here, the character corresponding to each cable is defined as the base of the gene. The environmental capacity, which is equivalent to the concept of the population size in genetic algorithms, is defined as the maximum allowable number of individuals per generation. If the population exceeds the environmental capacity, a portion of it will be eliminated based on the natural selection, until the population size equals the environmental capacity.

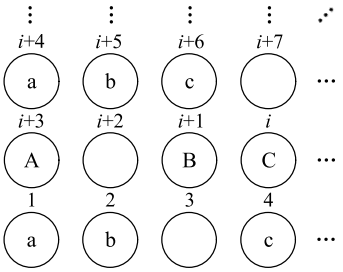

(a) diagram of a general cable arrangement, also known as a two-dimensional gene matrix.

a	b	0	c	⋯	C	B	0	A	a	b	c	0	⋯

(b) the corresponding sequence representation of the gene

FIGURE 2. The matrix and sequence representation of the gene for a duct bank installation composed of a number of ducts and several cables.

B. OPERATORS

The clone and mutation are probably the most natural evolution procedures for the CAP. Since the original mutation operator in [45] and [46] interchanges two completely random bases every time, which is somewhat crude, we propose an excitation operator and an interchange operator to replace the original one.

Before exciting bases, the excitation operator needs to identify all feasible base pairs that can be excited for interchange. The criterion for a feasible base pair is that the gene will change after the interchange of the two bases. In other words, the base pair composed of two identical bases (cables in the same phase and same load level) is not permitted to be excited. At the same time, it is stipulated that "0" bases cannot be used to form feasible base pairs with other bases (corresponding to the fact that empty ducts cannot be excited). It is obvious that the number of feasible base pairs in the proposed excitation process is less than the number of possible interchange pairs of the mutation process as given in [45] and [46]. This preprocessing ensures the real mutation of each offspring individual, thereby accelerating the evolution pace. Fig. 3 intuitively illustrates the feasible and infeasible base pairs.

Algorithm 1 Main Loop of Agamogenetic Algorithm

```
for t = 2 to M
    Q_t = P_{t-1}                          clone the parent population
    for i = 1 to N
        Q_t[i] = excitation (Q_t[i])       excite each individual of the offspring population
        Q_t[i] = interchange (Q_t[i])      interchange excited and/or "0" bases within each offspring
    E_t = P_{t-1} ∪ Q_t                    combine the parent and offspring population
    E_t = sort (E_t)                       sort in ascending order based on objective values
    P_t = E_t[1: N]                        reduce the extended population to environmental capacity
```

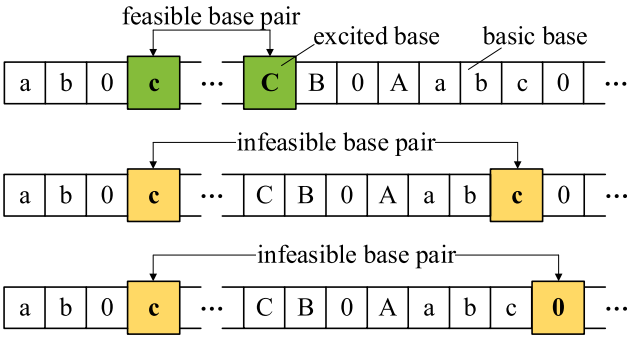

FIGURE 3. Examples of feasible and infeasible base pairs.

Among all feasible base pairs, the excitation operator randomly excites one base pair at a time, but the excited probability of each base pair is not equal, which is related to the excitation value of each base. The excitation value of each base is assigned according to its contribution to the objective function. For different grounding modes, there are usually different optimization goals, which result in the different assigned excitation values of the bases, thereby the different excited probabilities of feasible base pairs. This will be discussed in Section III in details.

The interchange operator is responsible for interchanging the excited bases and "0" bases. For cases without any empty duct, the two bases of the excited base pair just exchange their positions. For cases with empty ducts, however, the bases of the excited base pair have a certain probability to be interchanged with "0" bases. It is stipulated that the sum of the probabilities of an excited base being interchanged with all "0" bases is equal to the probability of the two excited bases interchanging. That is to say, when there is n "0" bases (corresponding to n empty ducts), the probability of an excited base interchanged with a random "0" base is one-nth of the probability of the two excited bases interchanging. The purpose of this stipulation is to prevent a decrease in the self-interchange probability of the excited base pair. Furthermore, not both bases of the excited pair may exchange positions with "0" bases. The criterion for determining whether an excited base can be exchanged with a "0" base is whether the interchange will have an impact on the objective function. For an excited pair, whether both bases in it are allowed to be interchanged with "0" bases, the probability of all allowed interchanges must be 1. When one excited base is interchanged with a random "0" base, the other one in the excited pair keeps its position unchanged and returns to the basic state.

For the first gene in Fig. 3, assuming that both excited bases are allowed to exchange positions with "0" bases, the probabilities of each interchange are illustrated in Fig. 4.

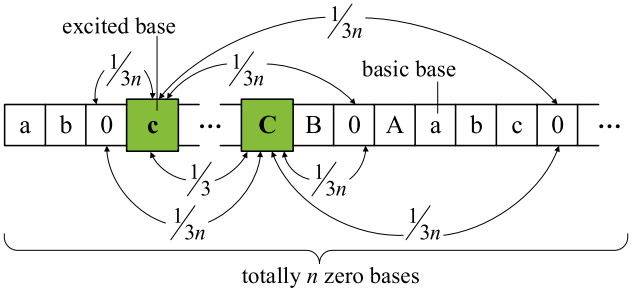

FIGURE 4. An example of the probability distribution of the interchange operator, where the fractions represent the interchange probability. This distribution is for the case that both excited bases are allowed to be interchanged with "0" bases.

C. MAIN LOOP

The main loop of the proposed agamogenetic algorithm consists of four procedures, which are clone, excitation, interchange, and sort. At first, the population P_1 composed of N individuals (corresponding to N genes) are initialized randomly. On this basis, the population undergoes (M-1) generations of evolutions. To maintain generality, we describe the evolutionary process of the proposed agamogenetic algorithm from the (t-1)th generation to the tth generation, of which the pseudo-code is shown at the top of the page.

Firstly, the (t-1)th-generation population P_{t-1} is copied into one clone. All individuals of the cloned population experience excitation and interchange operations, and constitute the offspring population Q_t of size N. Then, the parent population P_{t-1} and its offspring population Q_t are combined to form an extended population E_t, whose size is $2N$. Next, the extended population E_t is sorted based on the objective values of all individuals, and the top N individuals with good objective values constitute the tth-generation population P_t. Since all parent and offspring population members are included in E_t and are sorted together, elitism strategy is ensured, and the best individual is never lost in the

evolutionary process [47]. The iterative procedure of the proposed agamogenetic algorithm is also shown in Fig. 5.

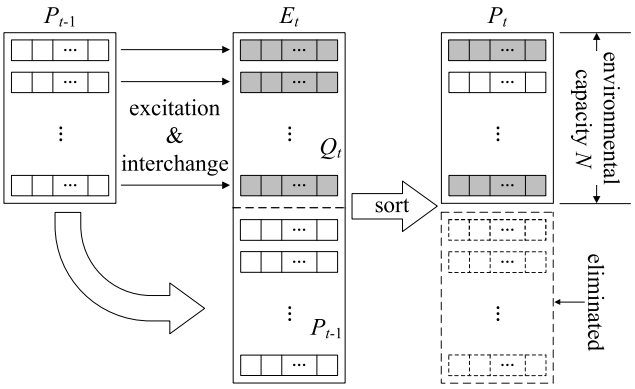

FIGURE 5. The iterative procedure of the agamogenetic algorithm, where the gene with shades of gray indicates that it has mutated.

III. ALGORITHM CUSTOMIZATIONS FOR DIFFERENT GROUNDING MODES

In this section, we discuss the customizations of the proposed agamogenetic algorithm for the two-ends grounding mode and the single-end grounding mode. It mainly involves the customizations of the excitation operator and the interchange operator. Due to different grounding modes and different optimization goals, the customizations are not exactly the same. We will elaborate on these customizations in the following subsections.

A. FOR TWO-ENDS GROUNDING MODE

For the two-ends grounding mode of cables in ducts, due to the huge circulating currents in metal sheaths, the optimization goal is set to minimize the total loss, including the core loss and the sheath loss, of the cable group. Based on this optimization goal, the excitation operator and the interchange operator are customized as follows.

The excitation operator firstly assigns an excitation value to each non-zero base. Since the total loss of the cable group is the summation of the loss of each cable, it is reasonable to choose the loss of each cable as its excitation value. However, due to the shielding effect of the metal sheaths, the core loss of each cable is almost unchanged regardless of the cable arrangement. Therefore, the core loss can be considered as ineffective contribution to the decrease of the objective value, and should be ignored in assigning excitation values to non-zero bases. It is only right and proper to use the sheath loss of each cable as its own excitation value, and the excitation probability of each non-zero base is defined as its excitation-value ratio, which is calculated by dividing the sheath loss of each cable by the total sheath loss of the cable group. In addition, using sheath loss as the excitation value makes sense. The higher the sheath loss, the more cables in the phase of the corresponding cable around it. Meanwhile, the higher the sheath loss, the greater the excitation probability of the corresponding cable, which leads to a larger probability of the corresponding cable to be exchanged to other positions, thereby to improve the situation of too many same-phase cables gathering. According to the principle of electromagnetic induction, the resultant induced electromotive force in the metal sheath tends to reduce, thereby to reduce the total sheath loss of the cable group. If the total loss of each cable is forcibly taken as its excitation value, because of the core loss of each cable being a large amount and almost the same with each other, the excitation probability of each non-zero base will tend to be equal, which loses the meaning of assigning excitation values to the cables.

After assignments of excitation values, the excitation operator picks up all feasible base pairs following the same criterion as mentioned in Section II-B, and at the same time to calculate the excitation probability of each feasible pair. The excitation probability of a feasible pair composed of the ith non-zero base and the jth non-zero base is formulated as:

$$p_i p_j \left(\frac{1}{1 - P_I} + \frac{1}{1 - P_J} \right), \tag{1}$$

where, p_i refers to the excitation probability of the ith non-zero base, p_j refers to the excitation probability of the jth non-zero base, P_I denotes the summation of the excitation probabilities of all bases identical to the ith non-zero base, P_J denotes the summation of the excitation probabilities of all bases identical to the jth non-zero base, subscript I represents the set of bases that are identical to the ith non-zero base, subscript J follows the same principle. It should be noted that P_I and P_J include the excitation probabilities of the ith and jth non-zero base, respectively. The summation of excitation probabilities of all feasible base pairs equals to 1, as demonstrated in Appendix.

After randomly exciting one base pair according to the probability distribution of feasible base pairs, the interchange operator starts mutating the gene. Regardless of which excited base changes its position, it will alter the loss of that cable, thereby affecting the total loss of the cable group. Therefore, both excited bases are allowed to interchange with "0" bases. Here, for the two-ends grounding mode, the probability of interchange between the two excited bases equals to 1/3, and the probability of interchange between either excited base and any "0" base equals to $1/(3n)$, where n refers to the number of "0" bases. The interchange probability distribution has been illustrated in Fig. 4.

B. FOR SINGLE-END GROUNDING MODE

For the single-end grounding mode of cables in ducts, due to the high sheath voltages, the optimization goal is set to minimize the maximum sheath voltage, thus to prevent the cable insulation from being penetrated. Therefore, the excitation operator and the interchange operator are customized in the following way.

Firstly, the excitation operator needs to assign excitation values to the non-zero bases. Since the optimization goal only involves the maximum sheath voltage, which means

that only the cable with the maximum sheath voltage contributes to the objective function, it is reasonable to assign an excitation value of 1 to the base corresponding to the maximum sheath voltage, and to assign an excitation value of 0 to any other non-zero base. This leads to the excitation probabilities of the feasible base pairs without the maximum-sheath-voltage base being zeros. For the feasible base pairs including the maximum-sheath-voltage base, the excitation probabilities are also zeros based on the assigned excitation values. However, in order to complete the excitation process, the excitation probabilities of the feasible base pairs including the maximum-sheath-voltage base cannot be zero. Therefore, we need to re-assign excitation values to the other excited base in the feasible pair with the maximum-sheath-voltage base. We choose the sheath voltage of the other excited base as its own excitation value, and the excitation-value ratios are defined as the excitation probabilities for each feasible pair that includes the maximum-sheath-voltage base respectively. It is noted that the re-assigned excitation value only works when the corresponding base constitutes a feasible pair with the maximum-sheath-voltage base. The customized excitation probability of each feasible base pair with the maximum-sheath-voltage base is formulated as:

$$V_i \Big/ \sum_{i=1}^{l} V_i, \tag{2}$$

where, V_i denotes the sheath voltage of the other excited base in the base pair including the maximum-sheath-voltage base, l represents the number of feasible base pairs that include the maximum-sheath-voltage base.

It is reasonable to define excitation probabilities as in (2). A cable has a higher sheath voltage because of more cables around in the phase of this central cable. Giving a higher excitation probability to this central cable increases the possibility of it being exchanged. Therefore, it is more likely to improve the situation of too many same-phase cables gathering, thereby reducing the resultant induced electromotive force in the sheath, which finally reduces the sheath voltages under the single-end grounding mode.

When the other excited base of an excited feasible pair that includes the maximum-sheath-voltage base is interchanged with a "0" base, owing to the exchanged base not corresponding to the maximum sheath voltage, this interchange has little or almost no contribution to the reduction of the optimization goal. According to the criterion for the interchange operator discussed in Section II-B, only the excited base corresponding to the maximum sheath voltage is allowed to be interchanged with "0" bases. Therefore, the self-interchange probability of the excited base pair is equal to 1/2, and the probability of the interchange between the maximum-sheath-voltage base and any "0" base is $1/(2n)$, where n refers to the number of "0" bases. For the first gene in Fig. 3, the interchange probability distribution under the single-end grounding mode is illustrated in Fig. 6.

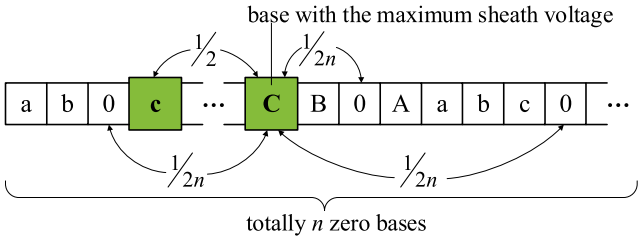

FIGURE 6. An example of the probability distribution of the interchange operator for the single-end grounding mode, where the fractions represent the interchange probability.

IV. GENERALIZED CROSS-BONDED GROUNDING MODE AND ITS OPTIMIZATION

For the cross-bonded grounding mode of power cables in ducts, the standard configuration in engineering is shown in Fig. 7, where the cables are arranged in a specific order, and the metal sheaths are only cross bonded within their own cable transmission circuit.

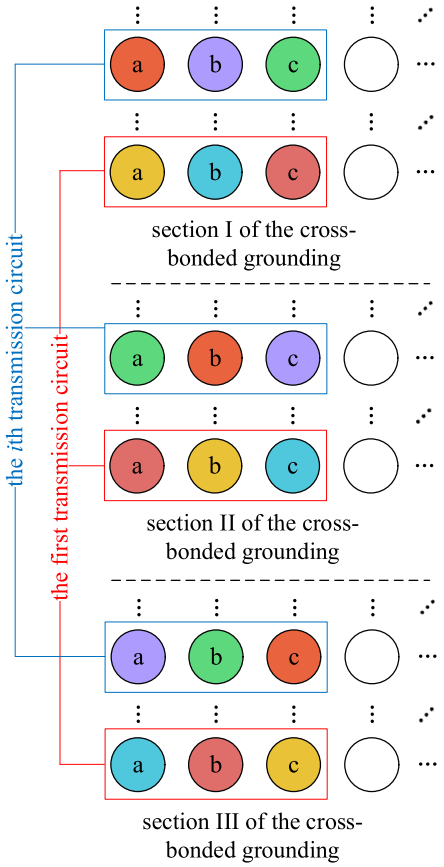

FIGURE 7. Diagram of the standard configuration of cables in ducts under the cross-bonded grounding mode, where the same colors represent the sheaths connected in series to form a circuit with the ground.

Owing to the ordered cable arrangement and sheath interconnection, obviously, the standard engineering configuration is unlikely to be the optimal configuration for the

minimum total loss of the cable group. There is a high probability that the irregular cable arrangements and the sheath interconnections between different transmission circuits can make the total loss smaller. Based on this understanding, we extend the standard cross-bonded grounding mode to the non-normalized form, namely the generalized cross-bonded grounding mode. In order to find the optimal configuration of the generalized cross-bonded grounding mode, we need to conduct deep customizations for the agamogenetic algorithm.

A. CUSTOMIZATION OF ENCODING

For the generalized cross-bonded grounding mode, there are not only the gene that records the cable arrangement in ducts, but also genes that record the cross connections of metal sheaths. This means that an individual here has four genes, which are one cable gene and three sheath genes corresponding to three sections of the grounding structure, respectively.

The cable gene is defined as mentioned above, which is a sequence consisting of character "0", "A", "B", "C", "a", "b", "c" and so on. The length of this character sequence is the number of ducts. The sheath gene has some differences. It is supposed that there are totally x cables in the duct bank. Because each sheath position is unique in each section of the grounding structure, it is reasonable to make each sheath correspond to a specific number between 1 and x. Consequently, each sheath gene is a full arrangement of numbers from 1 to x. The same number in different sheath genes means that the corresponding sheaths are connected in series. The positions from left to right in a sheath gene correspond to the cable positions along a specific route in the duct bank. The general sheath genes are illustrated in Fig. 8, where the position indexes above ducts and the position indexes above sheath-gene bases correspond, and the bases with the same number represent the sheaths connected in series. For example, the sheath in position "x-2" of section I, the sheath in position "x-1" of section II and the sheath in the first position of section III are connected in series.

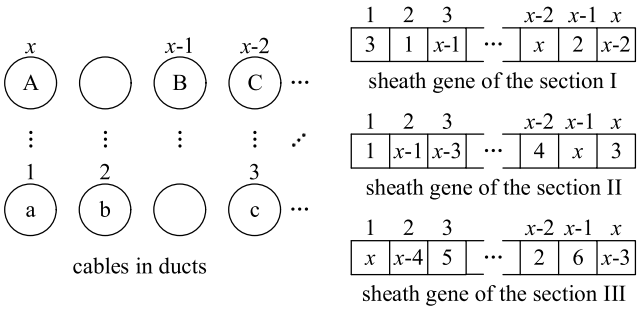

FIGURE 8. General sheath genes corresponding to three sections respectively.

B. CUSTOMIZATION OF OPERATORS

Due to different encoding methods of the cable genes and the sheath genes, the customizations of operators for the two types of genes are different. For the cable gene, the customized excitation operator in the generalized cross-bonded grounding mode is similar to that in the two-ends grounding mode, except for the chosen amount to use as the excitation value. Since the optimization goal is to minimize the total loss of the cable group, which is approximately equivalent to the minimization of the total sheath loss, we choose the total loss of the three sheaths corresponding to this cable as its excitation value. For instance, the excitation value of cable "A" at the position "x" in Fig. 8 is defined as the summation of the losses in the sheath "x-2" of section I, the sheath "3" of section II, and the sheath "x-3" of section III. The calculation formula of the excitation probability and the probability distribution of the interchange operator for the cable gene in the generalized cross-bonded grounding mode are identical to those in the two-ends grounding mode.

Unlikely that the sheath losses are just determined by the sheath's surrounding cable-core currents in the two-ends grounding mode, the sheath losses in the generalized cross-bonded grounding mode are also affected by the cross-bonded grounding structure. Although the sum of the three-section sheath losses of each cable cannot accurately reflect the crowding degree of the surrounding same-phase cables, it still reflects the irrationality of the cable arrangement to a certain extent. The larger the sum of the three-section sheath losses is, the more unreasonable the location of the corresponding cable is, and a larger excitation value should be assigned to the corresponding base to improve its excitation possibility, thereby to reduce the total sheath loss. To sum up, the summation of the three-section sheath losses of a same cable is a more proper index as the excitation value of the corresponding base.

For the sheath genes, the sheath loss is naturally chosen as the excitation value of the corresponding base. Larger sheath loss means that the three electromotive forces of the three sheaths in this sheath-ground circuit are more unbalanced. Meanwhile, the excitation value assignment makes it more possible to change the position of this certain base, thereby to have a probability to reduce the imbalance. Therefore, this excitation value assignment makes sense. Since there are no same bases or "0" bases in the sheath gene, any two bases can form a feasible base pair, thus there are totally $x(x\text{-}1)/2$ feasible base pairs in a sheath gene. At this point, the excitation probability of each feasible base pair is characterized as:

$$p_i p_j \left(\frac{1}{1-p_i} + \frac{1}{1-p_j} \right), \tag{3}$$

where, p_i refers to the excitation-value ratio of the ith base in the sheath gene, p_j refers to the excitation-value ratio of the jth base in the sheath gene, i is not equal to j. Due to the fact that a sheath is always attached to a cable and cannot be placed in an empty duct alone, the simultaneously excited two bases will be definitely exchanged.

Main Loop of the Customized Agamogenetic Algorithm for the Generalized Cross-Bonded Grounding Mode

```
for t = 2 to M
  Q_tc = P_{t-1}                                   clone the parent population
  for i = 1 to N
    Q_tc[i] = excitation (Q_tc[i], cable gene)      excite the cable genes of the offspring
    Q_tc[i] = interchange (Q_tc[i], cable gene)     interchange the excited cable gene within each offspring
  E_t = P_{t-1} ∪ Q_tc                             combine the parent and offspring population
  E_t = sort (E_t)                                 sort in ascending order based on objective values
  R_t = E_t[1: N]                                  form the middle population
  Q_ts1 = R_t, Q_ts2 = R_t, Q_ts3 = R_t            copy the middle population into three clones
  for i = 1 to N
    Q_ts1[i] = excitation (Q_ts1[i], sheath gene of section I)   excite section-I sheath gene of the first cloned population
    Q_ts1[i] =  interchange (Q_ts1[i], sheath gene of section I)
  for i = 1 to N
    Q_ts2[i] = excitation (Q_ts2[i], sheath gene of section II)
    Q_ts2[i] = interchange (Q_ts2[i], sheath gene of section II)
  for i = 1 to N
    Q_ts3[i] = excitation (Q_ts3[i], sheath gene of section III)
    Q_ts3[i] = interchange (Q_ts3[i], sheath gene of section III)
  S_t = R_t ∪ Q_ts1 ∪ Q_ts2 ∪ Q_ts3                combine middle population and its offsprings
  S_t = sort (S_t)
  P_t = S_t[1: N]                                  reduce the super extended population
```

C. CUSTOMIZATION OF THE MAIN LOOP

Due to different weights of cable genes and sheath genes in the optimization process, the customized main loop for the generalized cross-bonded grounding mode is divided into two stages, which are the evolution of the cable gene and the evolution of the sheath genes, respectively. Two stages are in a progressive relationship. Each stage consists of procedures of clone, excitation, interchange and sort. In the algorithm customization for the generalized cross-bonded grounding mode, the population P is composed of N individuals, each individual containing one cable gene and three sheath genes, and the population P undergoes totally M generations of evolution. The pseudo-code shown at the top of the page outlines the evolutionary process of the customized algorithm.

For the evolution of the cable gene, firstly, the (t-1)th-generation population P_{t-1} is copied into one clone. All individuals of the cloned population experience excitation and interchange operations only for the cable genes, with all sheath genes unchanged, and constitute the offspring population Q_{tc} of size N. Then, the parent population P_{t-1} and its offspring population Q_{tc} are combined to form an extended population E_t, whose size is $2N$. Next, the extended population E_t is sorted based on the objective values of all individuals, and the top N individuals with good objective values constitute the middle population R_t. These are the procedures of the first stage, which optimize the cable arrangements under the current established sheath-ground structure.

Based on the optimization results of the first stage, we carried out the optimization procedures of the second stage. At first, the middle population R_t is copied into three clones. All individuals of the first cloned population experience excitation and interchange operations only for the section-I sheath genes, with all other genes unchanged, and constitute the offspring population Q_{ts1} of size N. The offspring population Q_{ts2} only excites and interchanges the section-II sheath genes, with all other genes unchanged. The offspring population Q_{ts3} can be deduced by analogy. Then, the middle population R_t and its offspring populations Q_{ts1}, Q_{ts2} and Q_{ts3} are combined to form a super extended population S_t, whose size is $4N$. Next, the super extended population S_t is sorted based on the objective values of all individuals, and the top N individuals with good objective values constitute the tth-generation population P_t. By mutating only one-section sheath genes in one cloned population, the second stage can search the optimal cross-bonded configuration in a more methodical and effective way.

To sum up, through the two-stage strategy, the population is efficiently evolving in a positive direction. The customized main loop for the generalized cross-bonded ground mode is also shown in Fig. 9.

V. SIMULATION RESULTS

In this section, a real-life installation of cables in ducts is investigated, which consists of sixteen ducts and twelve cables including one heavy-load three-phase circuit and three light-load three-phase circuits. The purpose of the case study is to compare the performance of the agamogenetic algorithm with the VIS algorithm, as described in the only two literatures ([45], [46]) that genuinely and substantively optimize cable arrangements. These comparisons are made under the two-ends grounding mode and the single-end grounding mode respectively. Additionally, the case study aims to validate the effectiveness of the agamogenetic algorithm

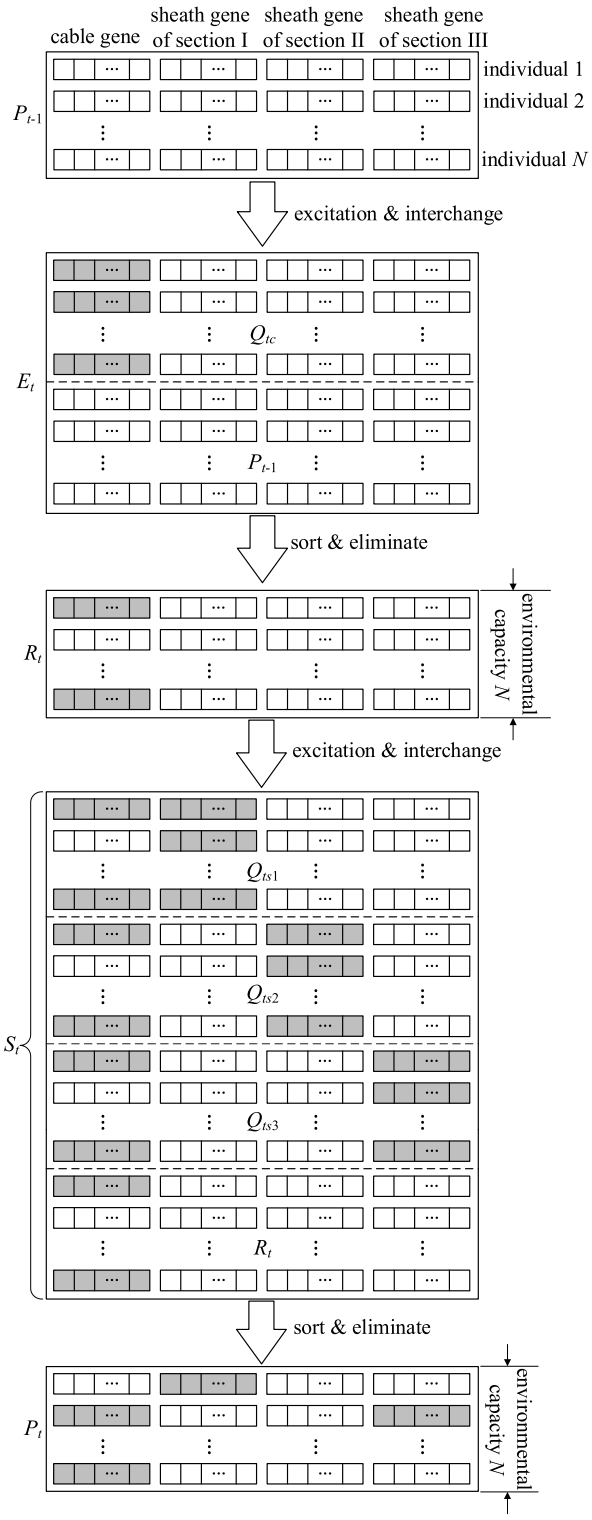

FIGURE 9. The customized iterative procedure of agamogenetic algorithm for the generalized cross-bonded grounding mode, where the gene with shades of gray indicates that it has mutated.

in optimizing the generalized cross-bonded grounding configuration.

The main loop of the VIS algorithm in [45] and [46] is the same as that of the agamogenetic algorithm in Fig. 5, except that the excitation and interchange processes are replaced by a completely random exchange process. For each of the first two grounding modes, we conduct six simulations for the two algorithms respectively, with the initial populations of six simulations for one algorithm are the same as those for the other algorithm respectively, to compare their optimization performance in a relatively fair way. In each simulation of both algorithms for the first two grounding modes, the population size and the number of generations are chosen to be: $N = 15$ and $M = 100$, respectively. In the simulation of the agamogenetic algorithm for the generalized cross-bonded grounding mode, the above parameters are set to be: $N = 50$ and $M = 50$. It is noted that we have not made any effort in finding the best parameter settings, just pick up them based on the experience. Numerical methods of electromagnetic fields are used to compute the objective values of each configuration. The load current of light-load cables is set to the effective value of 633 amperes, and the load current of heavy-load cables is set to the effective value of 799 amperes. At the beginning of the simulations for each grounding mode, we provide the standard engineering configuration and compute its objective value as reference.

A. FOR TWO-ENDS GROUNDING MODE

The standard engineering arrangement of cables in this duct bank for the two-ends grounding mode is shown in Fig. 10. Numerical results show that the standard arrangement for the two-ends grounding mode will lead to a total cable loss of 448.73 W/m, including the total core loss of 157.81 W/m and the total sheath loss of 290.92 W/m.

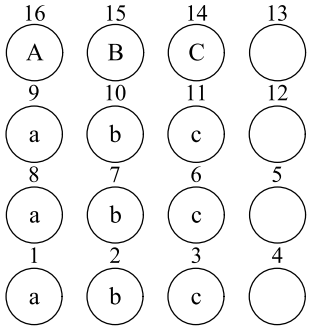

FIGURE 10. Diagram of the standard engineering arrangement in the chosen duct bank for the two-ends grounding mode.

The comparison of the convergence speed and convergence accuracy for the two algorithms is illustrated in Fig. 11. Although the agamogenetic algorithm has obviously higher computational complexity than the VIS algorithm, the actual computational times of both algorithms are identical. This is because the time consumption is mainly in the numerical calculation of electromagnetic fields of the tested configurations. By contrast, the time consumption of the algorithm itself can be ignored. Meanwhile, the averages of the optimal total losses derived from the agamogenetic algorithm and the VIS algorithm are 393.9449 W/m and 396.0651 W/m

respectively, where the former is 2.1202 W/m smaller than the latter. Therefore, it is shown in Fig. 11 that the agamogenetic algorithm can achieve better solutions in a higher speed compared with the VIS algorithm, which indicates that the agamogenetic algorithm converges faster and has a higher optimization accuracy. In addition, the variance of the optimal total losses found by the agamogenetic algorithm is 0.0256 $(W/m)^2$, smaller than that of the VIS algorithm, which is 0.9617 $(W/m)^2$. This indicates that the agamogenetic algorithm has a better convergence stability than the VIS algorithm. In summary, the above demonstrates the outperformance of the agamogenetic algorithm over the VIS algorithm for the two-ends grounding mode of CAP.

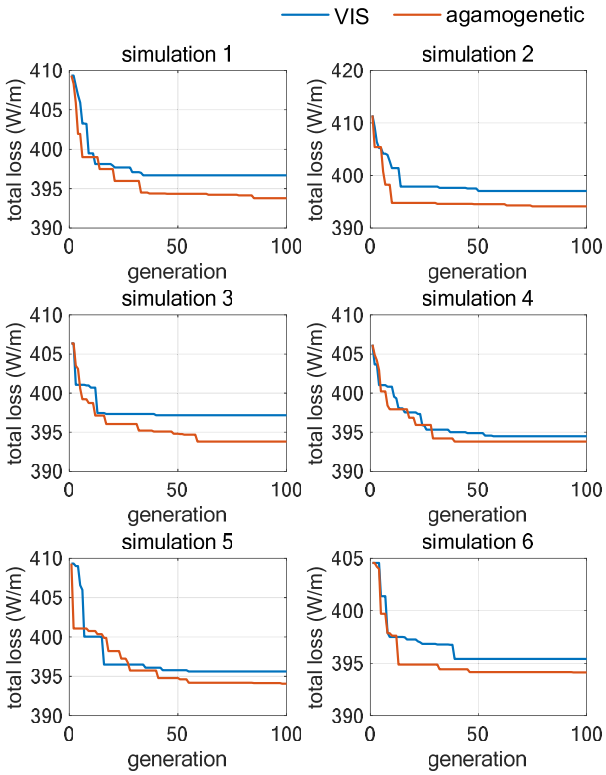

FIGURE 11. Performance comparison between the agamogenetic algorithm and the VIS algorithm under the two-ends grounding mode.

The optimal cable arrangement found among the six simulations of agamogenetic algorithm is "0 c a 0 c b a b a C A b 0 c B 0", which is shown in Fig. 12. The corresponding total cable loss is 393.7853 W/m, which includes the total core loss of 157.6793 W/m and the total sheath loss of 236.1060 W/m. This optimal total loss has decreased by 12.24% compared to that of the standard engineering arrangement. This large decrease illustrates the importance of selecting the proper cable arrangement in ducts under the two-ends grounding mode. The volumetric loss density distribution of the metal sheaths before and after optimization is shown in Fig. 13. It can be seen that, compared to the standard engineering arrangement, the optimization results of the agamogenetic algorithm significantly reduce the circulating current losses in the metal sheaths overall. This demonstrates the effectiveness of the proposed algorithm in suppressing circulating currents and their associated losses.

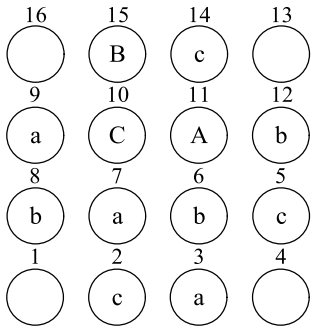

FIGURE 12. Diagram of the optimal cable arrangement found by the agamogenetic algorithm under the two-ends grounding mode.

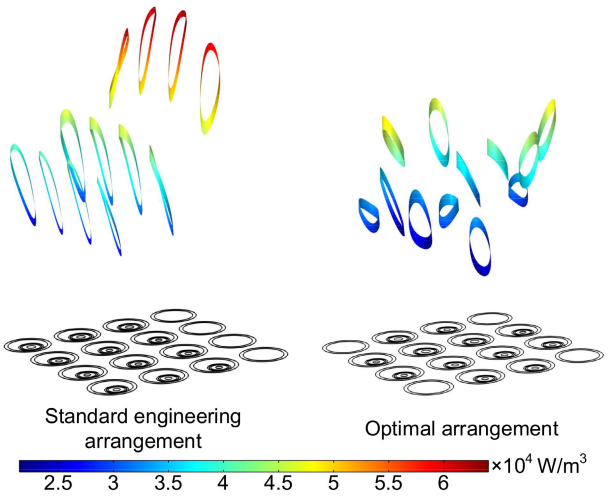

FIGURE 13. Volumetric loss densities of the metal sheaths for the standard engineering arrangement and the optimal arrangement found by the agamogenetic algorithm under the two-ends grounding mode.

B. FOR SINGLE-END GROUNDING MODE

The standard engineering arrangement of cables in the chosen duct bank for the single-end grounding mode is the same with that for the two-ends grounding mode (Fig. 10). Through numerical calculation, this arrangement results in a maximum sheath voltage of 109.74 V for a length of 500 meters, which corresponds to the cable located in duct 11.

The comparison of the convergence speed and convergence accuracy for the two algorithms is illustrated in Fig. 14. Similarly, the total computational time of 100 generations for each algorithm is almost the same. Meanwhile, the averages of the optimal maximum sheath voltages derived from the agamogenetic algorithm and the VIS algorithm are 54.76 V and 56.87 V respectively, where the former is 2.10 V smaller than the latter. Therefore, it is shown in Fig. 14 that the agamogenetic algorithm can achieve better solutions in a higher speed

compared with the VIS algorithm, which indicates that the agamogenetic algorithm converges faster and has a higher optimization accuracy for the single-end grounding mode. In addition, the variance of the optimal maximum sheath voltages found by the agamogenetic algorithm is 0.1836 V^2, smaller than that of the VIS algorithm, which is 0.9485 V^2. This indicates that the agamogenetic algorithm has a better convergence stability than the VIS algorithm. In summary, the above demonstrates the outperformance of the agamogenetic algorithm over the VIS algorithm for the single-end grounding mode of CAP.

The optimal cable arrangement found among the six simulations of agamogenetic algorithm is "0 b C a b 0 a 0 b c A c 0 B c a", as shown in Fig. 15. The maximum sheath voltage in this arrangement is 54.15 V for a length of 500 meters, which corresponds to the cable located in duct 3. This optimal maximum sheath voltage has decreased by 50.66% compared to that of the standard engineering arrangement. This tremendous decrease illustrates the importance of selecting the proper cable arrangement in ducts for the single-end grounding mode. The sheath voltages of each cable over 500 meters under the single-end grounding mode before and after optimization are shown in Fig. 16. It can be seen that, compared to the standard engineering arrangement, the optimal arrangement obtained by the agamogenetic algorithm significantly reduces the maximum sheath voltage in the duct bank and results in more balanced voltage magnitudes across the metal sheaths.

C. FOR GENERALIZED CROSS-BONDED GROUNDING MODE

The configuration of cables in the chosen duct bank for the standard cross-bonded grounding mode is shown in Fig. 17. Numerical results show that a complete cross-bonded configuration of the standard cross-bonded grounding mode has a total cable loss of 274.39 kW for a length of 1.5 km (each section being 500 meters long).

The optimal cable arrangement found by the agamogenetic algorithm is "a b c 0 0 b a c B C 0 A c b a 0", and the optimal cross-bonded sheath structures are "7, 11, 12, 3, 6, 8, 9, 1, 5, 2, 10, 4", "1, 5, 7, 4, 2, 11, 12, 3, 8, 9, 6, 10", and "9, 2, 5, 1, 11, 6, 8, 10, 12, 4, 7, 3" corresponding to three sections respectively. The optimal configuration is shown in Fig. 18. The corresponding total cable loss is 242.36 kW/(1.5km). This optimal total cable loss has decreased by 11.67% compared to that of the standard engineering configuration. This large decrease illustrates the importance of selecting the proper cable configuration in ducts for the generalized cross-bonded grounding mode. The volumetric loss density distribution of the metal sheaths in each section of the cross-bonded configuration before and after optimization is shown in Fig. 19. It is evident that by generalizing the standard cross-bonded grounding mode and optimizing its configuration using the agamogenetic algorithm, the losses in the metal sheaths are almost entirely eliminated. This thoroughly demonstrates the effectiveness

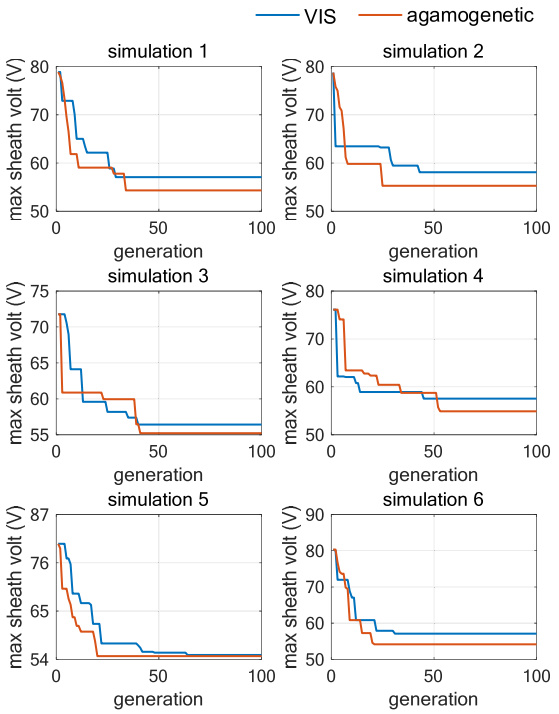

FIGURE 14. Performance comparison between the agamogenetic algorithm and the VIS algorithm under the single-end grounding mode.

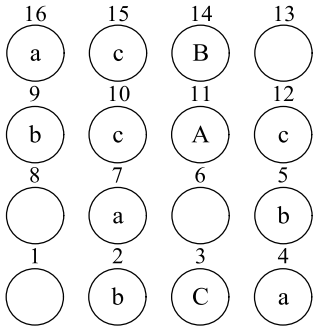

FIGURE 15. Diagram of the optimal cable arrangement found by the agamogenetic algorithm under the single-end grounding mode.

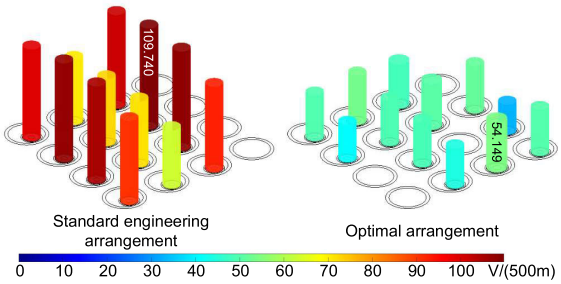

FIGURE 16. Sheath voltages over 500 meters for the standard engineering arrangement and the optimal arrangement found by the agamogenetic algorithm under the single-end grounding mode. The values indicate the maximum sheath voltages and their positions.

of the generalized cross-bonded grounding mode and the agamogenetic algorithm in suppressing circulating currents

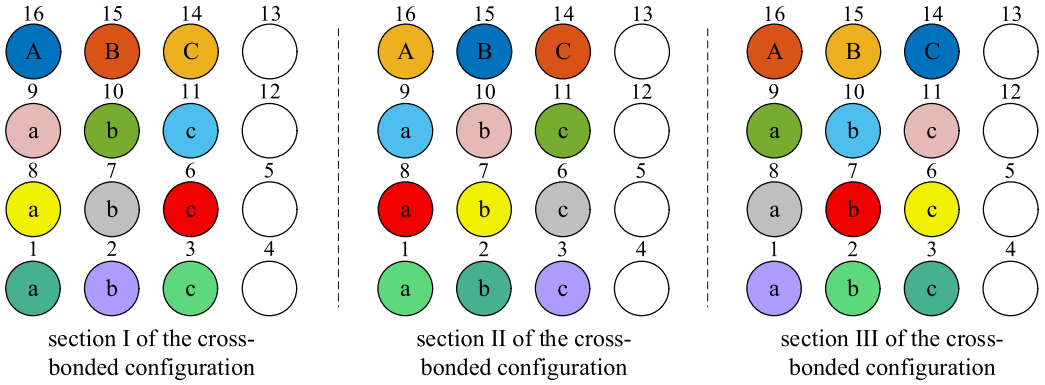

FIGURE 17. Configuration diagram of the standard cross-bonded grounding mode in the chosen duct bank, where the sheaths in the same-color ducts are connected in series.

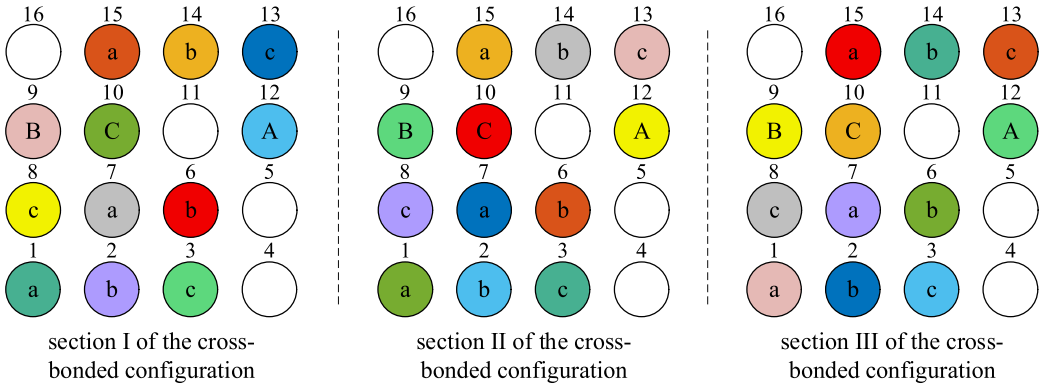

FIGURE 18. Diagram of the optimal configuration found by the agamogenetic algorithm for the generalized cross-bonded grounding mode, where the sheaths in the same-color ducts are connected in series.

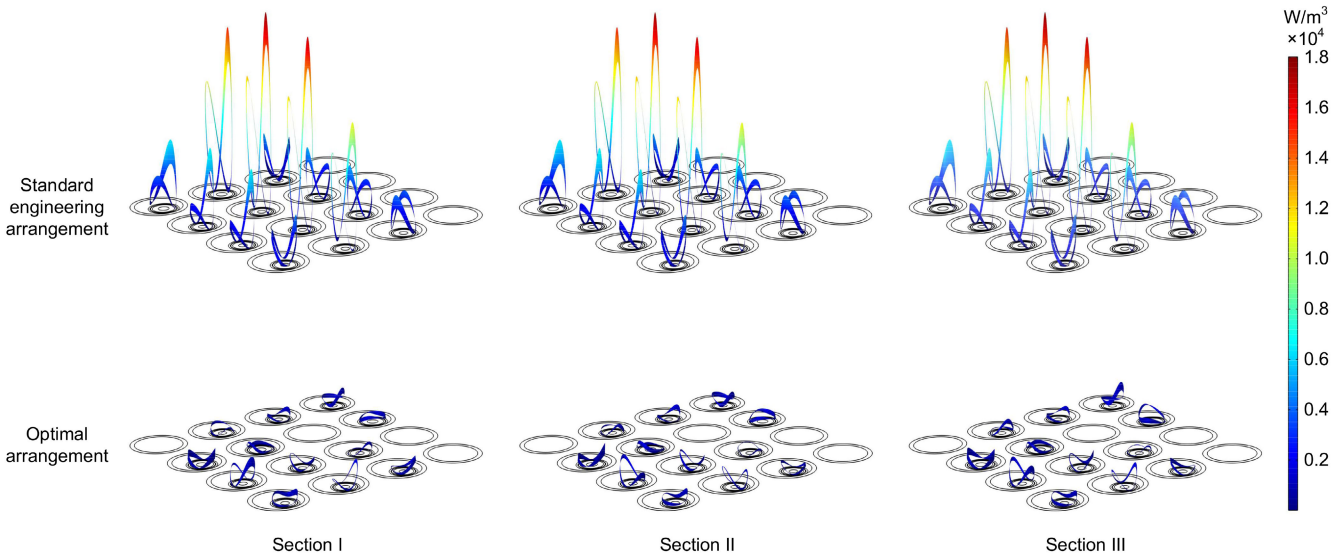

FIGURE 19. Volumetric loss densities of the metal sheaths for the configuration under the standard cross-bonded grounding mode and for the optimal configuration found by the agamogenetic algorithm under the generalized cross-bonded grounding mode.

and their associated losses in cross-bonded grounding. The convergence curve of the agamogenetic algorithm for the generalized cross-bonded grounding mode is illustrated in Fig. 20.

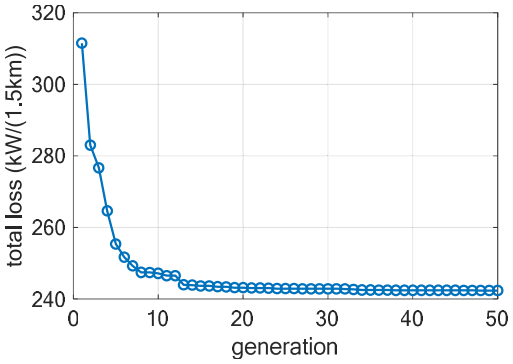

FIGURE 20. The convergence curve of the agamogenetic algorithm for the generalized cross-bonded grounding mode.

VI. CONCLUSION

This paper contributes two major achievements. Firstly, it proposes an efficient stochastic optimization algorithm, namely the agamogenetic algorithm, for optimizing cable arrangements in ducts, demonstrating higher accuracy and faster convergence speed compared to the existing optimization algorithm. Secondly, it generalizes the standard cross-bonded grounding mode for power cable groups in ducts and provides strategies for optimizing the cable arrangements and sheath connections of the generalized cross-bonded grounding mode using the proposed algorithm. Concretely, the proposed agamogenetic algorithm applies the roulette wheel selection strategy to the mutation process, creating two novel operators namely the excitation operator and the interchange operator. In the excitation operator, the concept of the feasible base pair is proposed to ensure the elimination of invalid mutations. Different feasible base pairs have different excitation probabilities, ensuring the efficiency of mutations. For the two-ends grounding mode and the single-end grounding mode respectively, the excitation operator and the interchange operator are customized to cope with the specific optimization goals of different grounding modes. Although there are some differences between the same operators in different grounding modes, the basic principles of them are the same. Thereafter, with the help of the agamogenetic algorithm, we are able to generalize the standard cross-bonded grounding mode, and optimize the generalized cross-bonded grounding configuration to minimize the total cable loss. The proposed algorithm is validated in a real-life duct bank installation comprising sixteen ducts and four three-phase circuits with different load levels. Numerical results show that the agamogenetic algorithm can find better solutions at a faster speed for both the two-ends and the single-end grounding modes, outperforming the VIS algorithm in the cable arrangement problem. Moreover, it is indicated that the agamogenetic algorithm has better convergence stability, with variance values of 0.0256 $(\mathrm{W/m})^2$ for two-ends grounding and 0.1836 V^2 for single-end grounding, compared to the VIS algorithm's 0.9617 $(\mathrm{W/m})^2$ for two-ends grounding and 0.9485 V^2 for single-end grounding. Simulation results also demonstrate that the optimal loss or voltage found by the agamogenetic algorithm decreases by 12.24% and 50.66% under the two-ends and single-end grounding modes, respectively, compared to the standard engineering arrangement. Furthermore, numerical results confirm the effectiveness of the agamogenetic algorithm in optimizing the generalized cross-bonded grounding configuration, with a total loss decrease of 11.67% compared to the standard engineering arrangement.

However, there are some limitations in the proposed algorithm. Due to the characteristics of the discrete optimization problem, the search results of the algorithm cannot always guarantee finding positions very close to the global optimum. Additionally, in several optimization simulations, the agamogenetic algorithm does not exhibit significant advantages over the existing method, such as in the fourth graph of Fig. 11 and the fifth graph of Fig. 14, where the optimization results are very similar to those of existing methods. This limitation could potentially be improved by designing more reasonable base excitation values or setting adaptive base excitation values.

APPENDIX

The sum of the excitation probabilities of all feasible base pairs derived from the set I and J is:

$$\sum_{i\in I}\sum_{j\in J} p_i p_j \left(\frac{1}{1-P_I}+\frac{1}{1-P_J}\right) = P_I P_J \left(\frac{1}{1-P_I}+\frac{1}{1-P_J}\right).$$

Assuming that all non-zero bases can be divided into m sets $\{I_1, I_2, \ldots, I_m\}$, each set containing only one type of base, the total excitation probability can be calculated as:

$$\begin{aligned}
&P_{I_1}P_{I_2}\left(\frac{1}{1-P_{I_1}}+\frac{1}{1-P_{I_2}}\right)\\
&\quad+P_{I_1}P_{I_3}\left(\frac{1}{1-P_{I_1}}+\frac{1}{1-P_{I_3}}\right)\\
&\quad+\cdots+P_{I_2}P_{I_3}\left(\frac{1}{1-P_{I_2}}+\frac{1}{1-P_{I_3}}\right)+\cdots\\
&\quad=\frac{P_{I_1}}{1-P_{I_1}}\left(P_{I_2}+P_{I_3}+\cdots+P_{I_m}\right)\\
&\quad+\frac{P_{I_2}}{1-P_{I_2}}\left(P_{I_1}+P_{I_3}+\cdots+P_{I_m}\right)+\cdots.
\end{aligned}$$

Considering the fact that the sum of excitation probabilities of all individual non-zero bases is 1, which is characterized as:

$$P_{I_1}+P_{I_2}+\cdots+P_{I_m}=1,$$

the expression of the total excitation probability can be simplified to

$$\begin{aligned}
&\frac{P_{I_1}}{1-P_{I_1}}\left(1-P_{I_1}\right)+\frac{P_{I_2}}{1-P_{I_2}}\left(1-P_{I_2}\right)\\
&\qquad+\cdots+\frac{P_{I_m}}{1-P_{I_m}}\left(1-P_{I_m}\right)=1.
\end{aligned}$$

Therefore, it is demonstrated that the total excitation probability of all feasible base pairs for the two-ends grounding mode equals 1.

REFERENCES

[1] A. Sedaghat, H. Lu, A. Bokhari, and F. de León, "Enhanced thermal model of power cables installed in ducts for ampacity calculations," *IEEE Trans. Power Del.*, vol. 33, no. 5, pp. 2404–2411, Oct. 2018, doi: 10.1109/TPWRD.2018.2841054.

[2] Y. Liang, "Steady-state thermal analysis of power cable systems in ducts using streamline-upwind/petrov-Galerkin finite element method," *IEEE Trans. Dielectr. Electr. Insul.*, vol. 19, no. 1, pp. 283–290, Feb. 2012, doi: 10.1109/TDEI.2012.6148529.

[3] Y. Liang, Z. Wang, J. Liu, Z. Xue, and Y. Li, "Numerical calculation of temperature field and ampacity of cables in ducts," *High Voltage Eng.*, vol. 36, no. 3, pp. 763–768, Mar. 2010, doi: 10.13336/j.1003-6520.hve.2010.03.032.

[4] Y. Liang, C. Yan, J. Zhao, K. Sun, and J. Liu, "Numerical calculation of transient temperature field and short-term ampacity of group of cables in ducts," *High Voltage Eng.*, vol. 37, no. 4, pp. 1002–1007, Apr. 2011, doi: 10.13336/j.1003-6520.hve.2011.04.029.

[5] G. J. Anders, M. Chaaban, N. Bedard, and R. W. D. Ganton, "New approach to ampacity evaluation of cables in ducts using finite elemet technique," *IEEE Trans. Power Del.*, vol. D-2, no. 4, pp. 969–975, Oct. 1987, doi: 10.1109/TPWRD.1987.4308208.

[6] X. Dong, Y. Yang, C. Zhou, and D. M. Hepburn, "Online monitoring and diagnosis of HV cable faults by sheath system currents," *IEEE Trans. Power Del.*, vol. 32, no. 5, pp. 2281–2290, Oct. 2017, doi: 10.1109/TPWRD.2017.2665818.

[7] C. H. Chien and R. W. G. Bucknall, "Analysis of harmonics in subsea power transmission cables used in VSC–HVDC transmission systems operating under steady-state conditions," *IEEE Trans. Power Del.*, vol. 22, no. 4, pp. 2489–2497, Oct. 2007, doi: 10.1109/TPWRD.2007.905277.

[8] D. A. Tziouvaras, "Protection of high-voltage AC cables," presented at the Power Syst. Conf., Adv. Metering, Protection, Control, Commun., Distrib. Resour., Clemson, SC, USA, 2006, pp. 316–328, doi: 10.1109/PSAMP.2006.285402.

[9] Z. Lei, X. Huang, T. Liu, and Y. Xu, "Analysis of an accident caused by current mismatch in the grounding structure of a high-voltage single-core submarine cable," presented at the IEEE 4th Int. Elect. Energy Conf. (CIEEC), Wuhan, China, 2021, doi: 10.1109/CIEEC50170.2021.9510303.

[10] Y. Xin, L. Jiang, X. Zhao, W. Li, J. Gao, B. Xi, L. Zhong, and L. Xia, "Cause analysis of aging ablation on sheath of 110 kV single core high voltage cable," presented at the IEEE Conf. Elect. Insul. Dielectric Phenomena (CEIDP), Richland, WA, USA, 2019, doi: 10.1109/CEIDP47102.2019.9009931.

[11] Y. Huang, Z. Zheng, Z. Lin, and Y. Zhang, "Fault analysis and corrosion at the lead seal of high-voltage cable joint," presented at the 18th Annu. Conf. China Electrotech. Soc. (ACCES), Singapore, 2023, pp. 35–45, doi: 10.1007/978-981-97-1428-5_5.

[12] S. Czapp and K. Dobrzynski, "Safety issues referred to induced sheath voltages in high-voltage power cables—Case study," *Appl. Sci.*, vol. 10, no. 19, p. 6706, Sep. 2020, doi: 10.3390/app10196706.

[13] Z. He, W. He, H. He, and J. Hong, "Study on the damage analysis of 110 kV cable structure," presented at the 5th Int. Conf. Power, Energy Mech. Eng. (ICPEME), Shanghai, China, 2021, pp. 1–6, doi: 10.1051/e3sconf/202124301006.

[14] M. Parol, J. Wasilewski, and J. Jakubowski, "Assessment of electric shock hazard coming from Earth continuity conductors in 110 kV cable lines," *IEEE Trans. Power Del.*, vol. 35, no. 2, pp. 600–608, Apr. 2020, doi: 10.1109/TPWRD.2019.2916890.

[15] P. C. J. M. van der Wielen, *On-Line Detection and Location of Partial Discharges in Medium-Voltage Power Cables*. Eindhoven, The Netherlands: Eindhoven Univ. Press, 2005, pp. 35–36.

[16] L. Chen, R. Xia, and J. Luo, "Technique research on the online detection and restraint of the induced voltage and circulating current on the metal sheath of 35kV 630 mm^2 single-core XLPE cable," presented at the CICED, Nanjing, China, 2010.

[17] V. Castorani, P. Cicconi, M. Mandolini, A. Vita, and M. Germani, "A method for the cost optimization of industrial electrical routings," *Comput.-Aided Des. Appl.*, vol. 15, no. 5, pp. 747–756, Mar. 2018, doi: 10.1080/16864360.2018.1441241.

[18] R. Ratchapan, S. Kriprab, S. Marsong, B. Plangklang, and Y. Kongjeen, "An analysis of the ampacity and capital costs for underground high voltage power cable construction methods," *Przegląd Elektrotechniczny*, vol. 100, no. 1, pp. 16–23, Jan. 2024, doi: 10.15199/48.2024.01.03.

[19] J.-M. Colef and F. de León, "Improvement of the standard ampacity calculations for power cables installed in trefoil formations in ventilated tunnels," *IEEE Trans. Power Del.*, vol. 37, no. 1, pp. 627–637, Feb. 2022, doi: 10.1109/TPWRD.2021.3068111.

[20] J. Liang, G. Feng, and Y. Tian, "Optimized arrangement of cables in cable tunnel of substation considering fireproof performance," presented at the IEEE Int. Conf. High Voltage Eng. Appl. (ICHVE), Chongqing, China, 2022, pp. 1–4, doi: 10.1109/ICHVE53725.2022.9961741.

[21] R. Benato, "Multiconductor analysis of underground power transmission systems: EHV AC cables," *Electr. Power Syst. Res.*, vol. 79, no. 1, pp. 27–38, Jan. 2009, doi: 10.1016/j.epsr.2008.05.016.

[22] Y. Liang, J. Huang, K. Jiang, and Z. Zhang, "Multiphysics coupling simulation and experimental study on temperature rise of high voltage cable laying in tunnel," presented at the Panda Forum Power Energy (PandaFPE), Chengdu, China, 2023, doi: 10.1109/PandaFPE57779.2023.10140592.

[23] R. M. Arias Velásquez and J. V. Mejía Lara, "New methodology for design and failure analysis of underground transmission lines," *Eng. Failure Anal.*, vol. 115, Sep. 2020, Art. no. 104604, doi: 10.1016/j.engfailanal.2020.104604.

[24] D. Fan, W. Liu, J. Huang, Y. Liang, and Z. Cheng, "Research on the influence of different arrangement schemes on the loss characteristics of 500kV AC cable," presented at the 2nd Asia Power Elect. Technol. Conf. (APET), Shanghai, China, 2023, pp. 192–195, doi: 10.1109/APET59977.2023.10489704.

[25] I. A. Metwally, A. H. Al-Badi, and A. S. Al Farsi, "Factors influencing ampacity and temperature of underground power cables," *Elect. Eng.*, vol. 95, no. 4, pp. 383–392, Nov. 2012, doi: 10.1007/s00202-012-0271-5.

[26] D. Fan, J. Huang, Z. Zhu, Y. Liang, and W. Liu, "High-voltage cable arrangement optimization design method," presented at the 8th Asia Conf. Power Elect. Eng. (ACPEE), Tianjin, China, 2023, doi: 10.1109/ACPEE56931.2023.10135648.

[27] Z. Zhang and Y. Wang, "Numerical simulation of 'thermal-mechanical' coupling of underground cable ducts," presented at the 3rd Int. Conf. Appl. Math., Modelling, Intell. Comput. (CAMMIC 2023), Tangshan, China, 2023, doi: 10.1117/12.2686034.

[28] S. Dubitsky, G. Greshnyakov, and N. Korovkin, "Refinement of underground power cable ampacity by multiphysics FEA simulation," *Int. J. Energy*, vol. 9, pp. 12–19, Jan. 2015.

[29] C. Che, B. Yan, C. Fu, G. Li, C. Qin, and L. Liu, "Improvement of cable current carrying capacity using COMSOL software," *Energy Rep.*, vol. 8, pp. 931–942, Nov. 2022, doi: 10.1016/j.egyr.2022.10.095.

[30] M. Mroz and G. J. Anders, "Optimization of cable layout with consideration of environmental impact," *IEEE Trans. Power Del.*, vol. 38, no. 6, pp. 4242–4252, Dec. 2023, doi: 10.1109/TPWRD.2023.3305484.

[31] J. Zhao, Q. Lei, Y. Fan, X. Deng, and S. Liu, "Optimization of ampacity for the unequally loaded power cables in duct banks," presented at the Asia–Pacific Power Energy Eng. Conf., Chengdu, China, 2010, doi: 10.1109/APPEEC.2010.5449351.

[32] H. Brakelmann and G. J. Anders, "A new method for analyzing complex cable arrangements," *IEEE Trans. Power Del.*, vol. 37, no. 3, pp. 1608–1616, Jun. 2022, doi: 10.1109/TPWRD.2021.3094666.

[33] Y. Fan, J. Zhao, K. Qian, S. Meng, F. Dou, and C. Peng, "Analysis and optimization for operation of the single-core power cables in parallel," *High Voltage Eng.*, vol. 36, no. 10, pp. 2607–2612, Oct. 2010, doi: 10.13336/j.1003-6520.hve.2010.10.042.

[34] H. Ren and S. Zheng, "Study on parameter unbalance of 500 kV double circuit cable line considering different arrangement," presented at the 4th Int. Conf. Energy, Elect. Power Eng. (CEEPE), Chongqing, China, 2021, doi: 10.1109/CEEPE51765.2021.9475678.

[35] Z. Zhang, X. Tang, Z. Chen, and H. Niu, "Research on joint optimization method for layout of pipeline cables," *Elect. Meas. Instrum.*, vol. 57, no. 15, pp. 8–13, Aug. 2020, doi: 10.19753/j.issn1001-1390.2020.15.002.

[36] H. Niu and R. Guo, "Position optimization of cables in ducts with FEM," presented at the Int. Conf. Condition Monit. Diagnosis (CMD), Xi'an, China, 2016, pp. 493–496, doi: 10.1109/CMD.2016.7757869.

[37] N. Duraisamy and A. Ukil, "Cable ampacity calculation and analysis for power flow optimization," presented at the Asian Conf. Energy, Power Transp. Electrific. (ACEPT), Singapore, 2016, doi: 10.1109/ACEPT.2016.7811535.

[38] B. Sun, "Study of cables in the distribution system: Parameters calculation, fault analysis, and configuration optimization," Ph.D. dissertation, Dept. Elect. Eng., Clemson Univ., Clemson, SC, USA, 2018.

[39] J. Wang, B. Liu, D. Li, X. Ma, B. Zhao, and Z. Yang, "Research on optimal placement methodology of power cable in ductbank," *Energy Rep.*, vol. 9, pp. 46–57, Mar. 2023, doi: 10.1016/j.egyr.2022.10.363.
[40] F. de Leon, "Major factors affecting cable ampacity," presented at the IEEE Power Eng. Soc. Gen. Meeting, Montreal, QC, Canada, 2006, doi: 10.1109/PES.2006.1708875.
[41] C. Fu, Y. Liang, J. Wang, Z. Zhao, and Y. Cui, "Transient temperature rise calculation for power cable in ducts under periodical current," presented at the 11th Int. Conf. Power Energy Syst. (ICPES), Shanghai, China, 2021, doi: 10.1109/ICPES53652.2021.9683988.
[42] P. Larranaga, C. M. H. Kuijpers, R. H. Murga, I. Inza, and S. Dizdarevic, "Genetic algorithms for the travelling salesman problem: A review of representations and operators," *Artif. Intell. Rev.*, vol. 13, no. 2, pp. 129–170, 1999, doi: 10.1023/A:1006529012972.
[43] H. Niu, Z. Chen, T. Yan, X. Tang, and C. Nie, "Optimization of tunnel multi-loop cable based on memetic algorithm," *J. South China Univ. Technol. (Natural Sci. Ed.)*, vol. 49, no. 10, pp. 141–150, Oct. 2021, doi: 10.12141/j.issn.1000-565X.200775.
[44] V. J. H. Jiménez, E. D. Castronuovo, and I. Sánchez, "Optimal statistical calculation of power cables disposition in tunnels, for reducing magnetic fields and costs," *Int. J. Elect. Power Energy Syst.*, vol. 103, pp. 360–368, Dec. 2018, doi: 10.1016/j.ijepes.2018.05.038.
[45] W. Moutassem and G. J. Anders, "Configuration optimization of underground cables for best ampacity," *IEEE Trans. Power Del.*, vol. 25, no. 4, pp. 2037–2045, Oct. 2010, doi: 10.1109/TPWRD.2010.2046652.
[46] A. Canova, F. Freschi, and M. Tartaglia, "Multiobjective optimization of parallel cable layout," *IEEE Trans. Magn.*, vol. 43, no. 10, pp. 3914–3920, Oct. 2007, doi: 10.1109/TMAG.2007.904456.
[47] K. Deb, A. Pratap, S. Agarwal, and T. Meyarivan, "A fast and elitist multiobjective genetic algorithm: NSGA-II," *IEEE Trans. Evol. Comput.*, vol. 6, no. 2, pp. 182–197, Apr. 2002, doi: 10.1109/4235.996017.

RUNZE CAI received the bachelor's degree in electrical engineering and automation from Hebei University of Technology, Tianjin, China, in 2016, and the master's degree in power electronics and power drives from the Institute of Electrical Engineering, Chinese Academy of Sciences, Beijing, China, in 2019. He is currently pursuing the Ph.D. degree in electrical engineering with Zhejiang University, Hangzhou, China.

SHIYOU YANG (Senior Member, IEEE) received the master's and Ph.D. degrees in electrical engineering from Shenyang University of Technology, Shenyang, China, in 1990 and 1995, respectively. He is currently a Professor and a Ph.D. Supervisor with the College of Electrical Engineering, Zhejiang University, Hangzhou, China. His research interests include numerical calculation and optimization of electromagnetic fields.